

Light-controlled release of caged doxorubicin from folate receptor-targeting PAMAM dendrimer nanoconjugate†

Seok Ki Choi,* Thommey Thomas, Ming-Hsin Li, Alina Kotlyar, Ankur Desai and James R. Baker, Jr.*

Received (in Cambridge, UK) 23rd December 2009, Accepted 22nd January 2010

First published as an Advance Article on the web 6th February 2010

DOI: 10.1039/b927215c

We report the synthesis and *in vitro* evaluation of folate receptor-targeted nanoconjugate that releases its therapeutic payload via a photochemical mechanism.

The targeted delivery of therapeutic and imaging agents using nanoconjugates is a burgeoning field.^{1–4} Strategies to develop cancer-cell specific nanoconjugates vary, but all attempts to selectively deliver therapeutics to cells use nanoscale carriers such as dendritic macromolecules,² liposomes,⁵ polymers,⁶ metal nanoparticles³ or viruses⁷ that include targeting and therapeutic agents. The desired result is less side toxicity in normal cells and more effective tumoricidal activity. Nanoconjugates also can be designed such that the therapeutic agents are released, and therefore active, only under particular conditions. The release mechanisms currently being explored are based primarily on reactions catalyzed by endogenous physiological factors such as reduction,¹ low pH,³ and hydrolytic enzymes.⁴ This communication describes a photochemical-based approach to release targeted drugs after delivery. In this scenario, the targeted drug conjugate is first placed on a surface, such as skin, or lung/gastrointestinal tract epithelium. After the exposure, the nanoconjugate drug is specifically taken up by the tumor cells and is washed away from the normal tissue; light is then applied from a laser device attached to an endoscope to specifically target the cancer cells. The strategy presented may be broadly applied to other cell targeting systems, particularly those that require time- and tissue-dependent control of drug activation.

Photocaging refers to the temporary inactivation of a biologically active molecule using a protective photocleavable group. Upon UV irradiation of the photocleavable group, the active form of the caged molecule is irreversibly released.⁸ Photocaging has been frequently applied *in vitro* towards the spatiotemporal control of biological processes^{9–11} and the light-triggered payload release from nanoscale materials.^{12,13} However, it has only been rarely applied in *in vivo* experiments^{14,15} because of the low level tissue penetration and phototoxicity associated with short wavelength UV light.

Recent advances in two-photon excitation^{14,15} and optical fiber technology, however, have made it possible to cleave

photocaged compounds by irradiation in the near-IR (720–800 nm¹⁴). Because of this potential for higher level tissue penetration, we have applied the photocaging approach towards the targeted delivery of doxorubicin,¹⁶ an anticancer drug that inhibits DNA replication through intercalation (Fig. 1).

In designing our photocage-based approach to the targeted delivery of therapeutics, we chose a fifth-generation (G5) polyamidoamine (PAMAM)¹⁷ dendrimer conjugated with folic acid (FA) ligands as the targeted carrier for the photocaged doxorubicin. This carrier system has been well studied and shown to undergo folate receptor (FAR)-mediated cellular internalization into cancer cells expressing up-regulated levels of the receptor.^{3,18–21} As a first synthetic step, a FAR-targeting ligand **1** was synthesized by performing an amide coupling of FA with ethylenediamine as a linker.²² A photocaged doxorubicin **5** was then synthesized after protection with an *ortho*-nitrobenzyl (ONB)-based photocleavable group **3** at its primary amine (Scheme 1).²² Both **1** and **5** were covalently coupled to carboxylic acid-terminated dendrimer **6**, G5 PAMAM-(glutaric acid)_{~100} ($M_n = 40\,850\text{ g mol}^{-1}$, PDI = $M_w/M_n \sim 1.046$),²² through amide formations (Scheme 2).

Crude nanoconjugate **7** obtained from the coupling reaction was purified by dialysis using membrane tubing (MWCO 10 kDa) to remove unreacted reactants and reagents. The conjugate **7** (G5-FA₈-Dox₄) was shown to have an average molar mass of 48 000 g mol⁻¹ (MALDI-TOF MS), and to contain an average of ~8 copies of **1** and ~4 copies of **5** per dendrimer molecule.²² Following the above synthetic strategy (Scheme 2), two fluorescein isothiocyanate (FITC)²³-labeled PAMAM doxorubicin conjugates²² **8** (G5-FA_{6,4}-Dox_{5,9}-FI_{1,2}) and **9** (G5-Dox_{5,9}-FI_{1,2}) were prepared either with or without FA ligand attached, respectively, in order to study them in cellular uptake experiments designed to probe FAR-mediated cell targeting.

The photochemical cleavage of ONB group-based linker **3** ($\lambda_{\text{max}} = 340\text{ nm}$, $\epsilon = 2750\text{ M}^{-1}\text{ cm}^{-1}$) was studied by exposing it in aqueous solution to UV-A light (Fig. 2(b)).²² Following

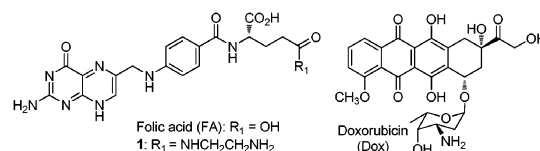
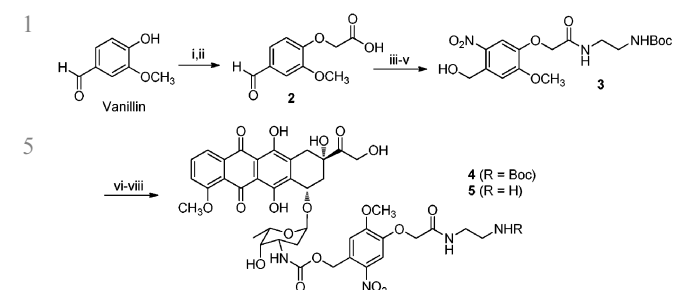


Fig. 1 Folic acid as a cancer targeting ligand, and doxorubicin as a chemotherapeutic agent.

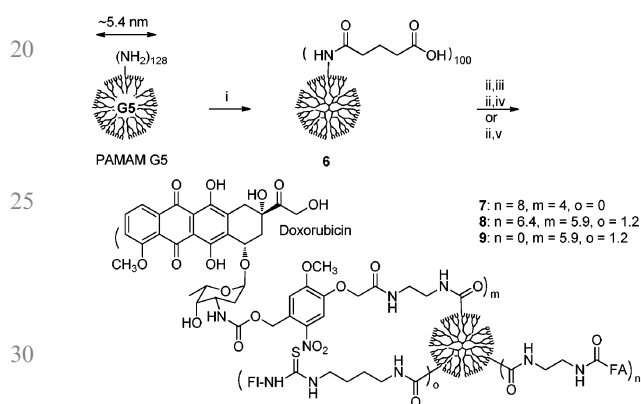
Michigan Nanotechnology Institute for Medicine and Biological Sciences, University of Michigan, Medical School, Ann Arbor, MI 48109, USA. E-mail: skchoi@umich.edu,

jbakerjr@med.umich.edu; Fax: (734) 615-0621; Tel: (734) 615-0618

† Electronic supplementary information (ESI) available: Experimental details for synthesis and characterization of **1–9**; details for photocleavage experiments of **3** and **7**. See DOI: 10.1039/b927215c



Scheme 1 Synthesis of doxorubicin-photocleavable linker **5**. *Reagents and conditions:* (i) ethyl bromoacetate, K_2CO_3 , DMF, rt, 17 h, 75%; (ii) NaOH, THF, MeOH, H_2O , rt, 33 h, 82%; (iii) conc. HNO_3 , AcOH, $0^\circ C$ to rt, 26 h, 68%; (iv) *N*-Boc-1,2-diaminoethane, DCC, DMAP, DMF, $0^\circ C$ to rt, 36 h, 88%; (v) $NaBH_4$, THF, MeOH, rt, 5 h, 71%; (vi) 4-nitrophenyl chloroformate, DIPEA, THF, $CHCl_3$, rt, 16 h, 98%; (vii) doxorubicin-HCl, Et_3N , DMF, rt, dark, 36 h, 72%; (viii) TFA, $CHCl_3$, rt, 15 min.



Scheme 2 Synthesis of PAMAM dendrimer conjugates **7–9**, including G5-FA-doxorubicin **7**, a folic acid-attached and doxorubicin-loaded fifth-generation polyamidoamine (PAMAM G5) dendrimer, in which doxorubicin is caged with a photocleavable *ortho*-nitrobenzyl group and tethered to the dendrimer surface. *Reagents and conditions:* (i) glutaric anhydride, Et_3N , MeOH, rt, 48 h; (ii) NHS, EDC, DMAP, DMF, rt, 36 h; (iii) FA- $CONHCH_2CH_2NH_2$ (**1**), doxorubicin-photocleavable linker (**5**), Et_3N , DMF, rt, 36 h; then H_2O , rt, 4 h; (iv) **1**, **5**, FITC- $NH(CH_2)_4NH_2$, Et_3N , DMF; then H_2O ; (v) **5**, FITC- $NH(CH_2)_4NH_2$, Et_3N , DMF; then H_2O .

irradiation, UV-vis absorption spectra taken showed a rapid decrease at 340 nm along with a concomitant increase at 270 nm (see ESI† for the plot of absorbance (340 nm) against irradiation time). This spectral change is attributable to the cleavage of the linker and the formation of nitrosobenzaldehyde⁸ as a byproduct at acceptable quantum efficiency ($\Phi = 0.29^{24}$). The UV-vis absorption spectroscopy of conjugate **7** and its irradiation time course are shown in Fig. 2(b). Prior to irradiation (bottom curve), **7** shows absorption features at long wavelengths that result from a weighted contribution of FA (absorption peaks: 280 nm, $\epsilon = 25\,545\ M^{-1}\ cm^{-1}$; 347 nm, $\epsilon = 6\,676\ M^{-1}\ cm^{-1}$), doxorubicin (480 nm, $\epsilon = 17\,376\ M^{-1}\ cm^{-1}$), and the linker **3**. The UV-vis time course of **7** indicates only insignificant changes in the absorption peaks attributable to FA, and doxorubicin. However, a large increase of absorbance around 280 nm was observed with $\sim 50\%$ of change at ~ 6 min, a

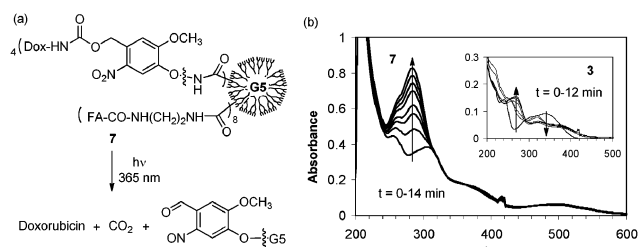


Fig. 2 (a) Photochemical release of doxorubicin from **7** by UV irradiation at 365 nm; (b) UV-vis spectral changes of **7** ($3.88\ \mu M$ in PBS, pH 7.2) as a function of irradiation time and those of **3** (inset; $33\ \mu M$ in 0.5% MeOH- H_2O) indicating the rapid generation of *ortho*-nitrosobenzaldehyde chromophore.

spectral feature that was observed analogously in the photolysis of the ONB linker **3** (inset). Analysis of the irradiated solutions of conjugate **7** by analytical reversed phase HPLC also confirmed time-dependent release of doxorubicin.²²

The cellular binding and uptake of PAMAM dendrimer doxorubicin conjugates **8** (with FA ligand attached), and **9** (without FA attached) were measured in KB cells expressing a high level of folate receptor²⁵ (Fig. 3(a)). The FA-bearing conjugate **8** bound to the cells in a dose-dependent manner, reaching a maximum association at 100 nM, while those conjugates without FA (**9**, G5-FITC²⁵) did not show any significant level of cellular association. Ligand specificity in the cellular uptake of **8** in the KB cells was studied by competitive binding experiments performed in the presence of free FA (Fig. 3(b)), which suggested the FA ligand-specific uptake of **8**. The FAR-mediated cellular uptake was further confirmed by confocal microscopy (Fig. 3(c)), showing that **8** only underwent the cellular uptake in a FA-competitive manner as indicated by the intracellular localization of its green fluorescence (FITC). A *z*-series analysis confirmed the intracellular localization of **8** (data not shown). The combined results based on the saturable binding of **8**, its competitive inhibition by free FA, and the confocal microscopy analysis clearly indicate FAR-specific binding and internalization of the FA-presenting dendrimer doxorubicin conjugate.

We tested the *in vitro* cytotoxicity of conjugate **7** using a FAR-over-expressing KB cell-based assay.¹⁸ As shown in Fig. 4, conjugate **7** (filled triangle) was inactive prior to UV irradiation (light exposure, 0 min), but inhibited cell growth after exposure to UV light as a function of irradiation time. Maximum inhibition of cell proliferation was observed following 30 min irradiation ($\sim 80\%$ reduction in cell growth), a level that is comparable to free doxorubicin ($\sim 85\%$, filled square). Fig. 4 also shows the cytotoxic activity of doxorubicin and PBS, positive and negative controls, respectively, under identical conditions. Free doxorubicin showed slightly decreased activity ($\sim 70\%$ inhibition) at the 30 min time point, perhaps as a result of UV-induced inactivation.²⁶ These results suggest that the doxorubicin-caged nanoconjugate **7** is only cytotoxic to the target KB cells once it has been exposed to UV light, and the doxorubicin has been released.

In summary, we have demonstrated the light-controlled release of doxorubicin from a FAR-targeted PAMAM nanoconjugate. This dual mechanism approach to drug delivery (cell targeting and photocontrolled release) could be more

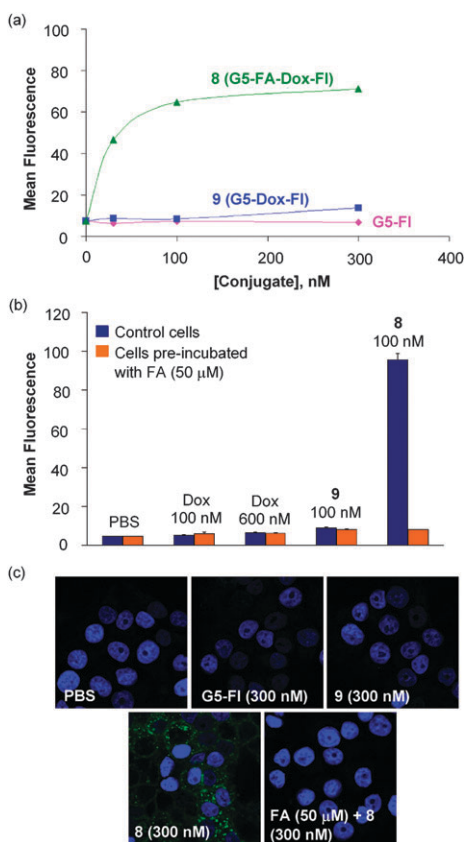


Fig. 3 (a) Dose-dependent binding of PAMAM dendrimer conjugates **8**, **9** and G5-FITC²⁵ in KB cells. The cells were incubated with each of the conjugates at varying concentrations for 2 h, rinsed and measured for its mean fluorescence in a flow cytometer; (b) Effect of free FA (50 μ M) on the uptake of **8** and **9** in KB cells; (c) Confocal microscopy of KB cells treated with **8**, **9** or G5-FITC. KB cells were incubated with each of the indicated conjugates for 2 h, fixed and treated with a nuclear staining agent, DAPI (4',6-diamidino-2-phenylindole). Some cells (bottom right) were pre-incubated with free FA for 15 min prior to incubation with **8**. The DAPI (blue) and FITC (green) fluorescence were measured using a confocal microscope.

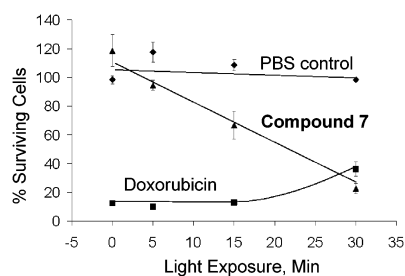


Fig. 4 Time-dependent, UV light-controlled activation of doxorubicin-caged **7** and induction of cytotoxicity. KB cells were exposed to UV light (365 nm) in phosphate buffered saline (PBS) containing 0.1% bovine serum albumin in the presence of compound **7** or doxorubicin at 3 μ M (per a doxorubicin basis in **7**), or PBS alone for different time periods. After incubation for 5 days following irradiation, cytotoxicity was quantified by a colorimetric assay based on XTT (sodium 3-[1-(phenylaminocarbonyl)-3,4-tetrazolium]-bis(4-methoxy-6-nitro)-benzene sulfonic acid hydrate). The data shown are the mean \pm SE of eight replicate cell samples from a representative experiment.

effective at enhancing the therapeutic index of an anticancer drug than either mechanism alone. We believe that this dual strategy is of particular value for those therapeutic applications that require non-invasive and spatiotemporal drug activation. Future efforts to enhance the scope of potential *in vivo* applications will focus on investigating the use of longer wavelength light and two-photon excitation.^{14,15,27}

This work was supported by the National Cancer Institute, National Institutes of Health under award 1 R01 CA119409 (J. R. B.). We thank Dr Pascale Leroueil for her expert proofreading of the manuscript.

Notes and references

- I. Ojima, *Acc. Chem. Res.*, 2008, **41**, 108–119.
- I. J. Majoros, C. R. Williams and J. James R. Baker, *Curr. Top. Med. Chem.*, 2008, **8**, 1165–1179.
- R. P. Feazell, N. Nakayama-Ratchford, H. Dai and S. J. Lippard, *J. Am. Chem. Soc.*, 2007, **129**, 8438–8439.
- G. M. Dubowchik and M. A. Walker, *Pharmacol. Ther.*, 1999, **83**, 67–123.
- R. J. Lee and P. S. Low, *Biochim. Biophys. Acta, Biomembr.*, 1995, **1233**, 134–144.
- I. Brigger, C. Dubernet and P. Couvreur, *Adv. Drug Delivery Rev.*, 2002, **54**, 631–651.
- G. Destito, R. Yeh, C. S. Rae, M. G. Finn and M. Manchester, *Chem. Biol.*, 2007, **14**, 1152–1162.
- G. Mayer and A. Heckel, *Angew. Chem., Int. Ed.*, 2006, **45**, 4900–4921.
- E. A. Lemke, D. Summerer, B. H. Geierstanger, S. M. Brittain and P. G. Schultz, *Nat. Chem. Biol.*, 2007, **3**, 769–772.
- T. Furuta, S. S. H. Wang, J. L. Dantzker, T. M. Dore, W. J. Bybee, E. M. Callaway, W. Denk and R. Y. Tsien, *Proc. Natl. Acad. Sci. U. S. A.*, 1999, **96**, 1193–1200.
- K. H. Link, Y. Shi and J. T. Koh, *J. Am. Chem. Soc.*, 2005, **127**, 13088–13089.
- N. K. Mal, M. Fujiwara and Y. Tanaka, *Nature*, 2003, **421**, 350–353.
- S. S. Agasti, A. Chomposor, C.-C. You, P. Ghosh, C. K. Kim and V. M. Rotello, *J. Am. Chem. Soc.*, 2009, **131**, 5728–5729.
- N. Gagey, P. Neveu and L. Jullien, *Angew. Chem.*, 2007, **119**, 2519–2521.
- H. A. Collins, M. Khurana, E. H. Moriyama, A. Mariampillai, E. Dahlstedt, M. Balaz, M. K. Kuimova, M. Drobizhev, X. D. YangVictor, D. Phillips, A. Rebane, B. C. Wilson and H. L. Anderson, *Nat. Photonics*, 2008, **2**, 420–424.
- M. Cirilli, F. Bachechi, G. Ughetto, F. P. Colonna and M. L. Capobianco, *J. Mol. Biol.*, 1993, **230**, 878–889.
- D. A. Tomalia, A. M. Naylor and I. William A. Goddard, *Angew. Chem., Int. Ed. Engl.*, 1990, **29**, 138–175.
- I. J. Majoros, T. P. Thomas, C. B. Mehta and J. R. Baker, *J. Med. Chem.*, 2005, **48**, 5892–5899.
- I. J. Majoros, A. Myc, T. Thomas, C. B. Mehta and J. R. Baker, *Biomacromolecules*, 2006, **7**, 572–579.
- Dendrimer-Based Nanomedicine*, ed. I. Majoros and J. James Baker, Pan Stanford, Hackensack, NJ, 2008.
- P. S. Low, W. A. Henne and D. D. Doorneweerd, *Acc. Chem. Res.*, 2008, **41**, 120–129.
- See ESI† for full details.
- G. R. Gapski, J. M. Whiteley, J. I. Rader, P. L. Cramer, G. B. Hendersen, V. Neef and F. M. Huennekens, *J. Med. Chem.*, 1975, **18**, 526–528.
- Quantum efficiency was estimated according to a method described in: P. J. Serafinowski and P. B. Garland, *J. Am. Chem. Soc.*, 2003, **125**, 962–965.
- T. P. Thomas, I. J. Majoros, A. Kotlyar, J. F. Kukowska-Latallo, A. Bielinska, A. Myc and J. R. Baker, *J. Med. Chem.*, 2005, **48**, 3729–3735.
- A. J. Carmichael and P. Riesz, *Arch. Biochem. Biophys.*, 1985, **237**, 433–444.
- J. R. R. Majjigapu, A. N. Kurchan, R. Kottani, T. P. Gustafson and A. G. Kutateladze, *J. Am. Chem. Soc.*, 2005, **127**, 12458–12459.